metals

Article

Assessing Tensile Strength and Electrical Conductivity of Friction Stir-Welded Joints of Copper and Aluminum Alloys

Elizabeth Hoyos *, **María Camila Serna**, **Yesid Montoya** and **Jorge Hernán Córdoba**

Department of Mechanical Engineering, Universidad EIA, Envigado 055428, Colombia; maria.serna14@eia.edu.co (M.C.S.); yesid.montoya@eia.edu.co (Y.M.); jorge.cordoba94@eia.edu.co (J.H.C.)
* Correspondence: elizabeth.hoyos@eia.edu.co

Abstract: Dissimilar aluminum joints have widespread applications across various industries, including the electronics and automotive sectors, owing to their unique combination of advantages, including reduced density and enhanced mechanical properties. These characteristics make them an innovative solution for multi-material processing challenges presented in the engineering industry. This article focuses on Friction Stir-Welded butt joints made using a weld–flip–weld approach between aluminum AA6061-T6 and pure copper C11000, exploring the effects of varying rotational speeds (1000, 1200, and 1400 RPM), offsets (0 and 1 mm) in the joint soundness, mechanical strength, and electrical conductivity. The welds were evaluated using non-destructive testing with phased-array ultrasound and tensile testing. Additionally, the electrical conductivity was measured to assess their response to electrical currents. The findings reveal a significant correlation between joint efficiency and electrical conductivity, with the highest values corresponding to a weld executed with a rotational speed of 1400 rpm, traverse speed of 40 mm/min, and 1 mm offset towards the aluminum, achieving the highest joint efficiency, reaching a joint efficiency of approximately 75% and 82.42% of the IACS for electrical conductivity.

Keywords: friction stir welding; dissimilar joints; butt joints; aluminum; copper

Citation: Hoyos, E.; Serna, M.C.; Montoya, Y.; Córdoba, J.H. Assessing Tensile Strength and Electrical Conductivity of Friction Stir-Welded Joints of Copper and Aluminum Alloys. *Metals* **2024**, *14*, 631. https://doi.org/10.3390/met14060631

Academic Editors: Abdelmageed A. Elmustafa, Rajiv S. Mishra and Yufeng Sun

Received: 16 March 2024
Revised: 17 May 2024
Accepted: 18 May 2024
Published: 26 May 2024

1. Introduction

Friction Stir Welding (FSW) is a solid-state welding process that was patented in 1991 by The Welding Institute (TWI). It is performed by utilizing a non-consumable cylindrical tool that rotates and advances in the material to be welded. These movements produce heat through friction and mix the softened material to produce the weld [1]. The tool comprises a shoulder that generates heat and exerts downward forging force and a probe that transports plasticized material along the joint [2].

FSW presents numerous advantages over conventional fusion welding methods, since it occurs at temperatures below the melting point of the material, such as minimizing distortion in the workpiece and reducing porosity and cracking when compared to traditional welding techniques. Additionally, FSW stands out as an environmentally conscious technology, and is often regarded as a "green" solution due to its reduced energy consumption compared to fusion processes. It does not require filler material or the use of solvents [3].

For the execution of FSW, various types of equipment can be utilized, all of which need to be robust enough to manage the diverse forces encountered during welding, such as axial force, traverse force, side force, and torque. This equipment range includes adapted conventional machine tools, dedicated FSW machines, custom-built machines, and industrial robots. Since FSW shares similarities with manufacturing processes like machining, deburring, grinding, and drilling, it is feasible to perform FSW on a conventional machine with certain modifications. These modifications, which are necessary to handle the high loads produced during FSW, might include the installation of sensors, structural reinforcement, or the addition of extra motors to enhance the machine's strength and stiffness [4,5]. FSW offers the ability to weld low-weldability alloys, which is the case with aluminum and titanium, amongst others. Some authors, such as Zhang et al. [6] and Nandan et al. [7], are investigating the potential of joining dissimilar materials. In various engineering applications, dissimilar materials, including metals and polymers, are strategically combined to harness the distinct mechanical properties of each component. This approach creates hybrid properties on two different fronts, leveraging differences in density to structure lighter materials or adapt them to reduce manufacturing costs in the market.

The use of dissimilar materials results in enhanced system performance and cost reduction, making it a top-notch engineering solution in multi-material processing. Dissimilar welding techniques have succeeded across various sectors, including automotive, electronics, aerospace, and numerous engineering domains [8–10]. Notably, the electrical industry has begun embracing this approach, and this is particularly evident in applications within generation, storage, and transmission systems. Additionally, in automation, notable instances of the use of these materials include the fabrication of electric motor cages [11]. When seeking to obtain dissimilar joints, Friction Stir Welding (FSW) is an interesting alternative, and the selection of appropriate parameters for this purpose is a task of interest. Seeking to identify process parameters in the development of FSW in aluminum–copper joints, authors such as Mehta et al. developed a review on dissimilar joints using these materials. The article includes information regarding the tool, its process parameters, and its mechanical properties [12]. Moreover, Al-Jarrah et al. [13] performed butt welds on pure copper and aluminum 6061 using a square pin and flat shoulder as the welding tool. They utilized process parameters of 60 mm/min and 1118 rpm, resulting in an ultimate tensile strength (UTS) of approximately 140 MPa. As a reference, authors such as Ahmadi et al. investigated a homogeneous AA6061 joint, achieving an ultimate tensile strength of 208 MPa with a square pin using 1200 RPM and 120 mm/min [14].

In the article written by Chowdhury et al. [15], the authors investigated the resulting mechanical properties by joining dissimilar metals of 6063 aluminum alloy and copper alloy using Friction Stir Welding (FSW) and Ultrasonic-Assisted Friction Stir Welding (UAFSW). The maximum efficiency was obtained using a combination of 500 rpm and 25 mm/min. Furthermore, Karrar et al. [16] carried out investigations on the effects of tools' rotational and traversal speeds on dissimilar friction stir butt welds on 3 mm thickness AA5083 to pure copper plates. The authors found that the highest efficiency achieved was 94.8%, using process parameters of 1400 RPM and 120 mm/min. Using the previous information and due to the extensive applications and advantages of FSW, this work focuses on the dissimilar FSW of aluminum AA 6061-T6 alloy and pure copper C11000 sheets. The mechanical characteristics that resulted from the dissimilar joints were investigated. Furthermore, non-destructive testing (NDT) was carried out.

The current study builds upon the previously mentioned information, shaping the foundation of this topic. In the following sections, we reference the methodology and materials employed. Utilizing a basic experimental design approach, the study engages in a comprehensive discussion on how the process parameters influence the properties of the welds produced.

2. Materials and Methods

2.1. Experimental Setup

Our study involved the production of butt-welded specimens utilizing aluminum alloy AA6061-T6 and copper C11000, each with dimensions of 150 mm $\times$ 50 mm $\times$ 4.76 mm, as illustrated in Figure 1a,b. The material compositions are in Table 1. Table 2 includes the electrical conductivity of the materials in terms of % IACS. This term refers to the International Annealed Copper Standard, which provides a baseline for comparing the electrical conductivity of various materials with that of annealed copper [17]. The tool used featured a concave shoulder of 27 mm in diameter and a threaded cylindrical probe with a 5 mm diameter. The advancing side, where the FSW tool actively stirred and plasticized the material, was made of aluminum, while the retracting side was copper. This information was based on findings by authors such as Eslami et al., Yusof et al., and Argesi et al., which illustrated the production of sound weld joints using this configuration [18–20].

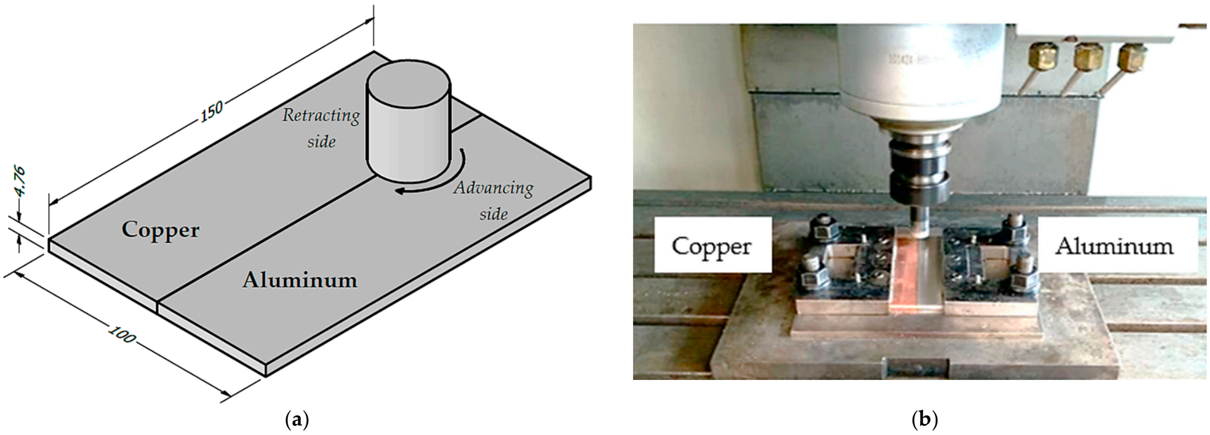

Figure 1. Welding setup. (**a**) Configuration of joint. (**b**) Fixture used for execution of welding.

Table 1. Materials composition. Adapted from Ref. [21].

Material	Si	Cu	Zn	Fe	Mn	Cr	Sn	Ti	Mg	Others
AA6061-T6	0.4	0.16	0.025	0.7	0.15	0.04	0.05	0.15	0.8	95.8
C11000	-	99.9	-	-	-	-	-	-	-	0.1

Table 2. Electrical conductivity experimentally measured on base materials.

Material	Electrical Conductivity in Terms of % IACS
AA6061-T6	39
C11000	97

The FSW process was carried out using a FIRST MCV-1100 CNC machine with a FANUC 18i-MB controller. It is noteworthy that this CNC machine is primarily used for traditional machining operations like milling; however, the force involved during the execution of FSW is significantly higher [4]. In order to prevent equipment damage, the welding was performed using a "weld–flip–weld" sequence, which involved welding with partial penetration, flipping the base materials, and welding again to achieve complete penetration. Figure 2 presents a simple schematic.

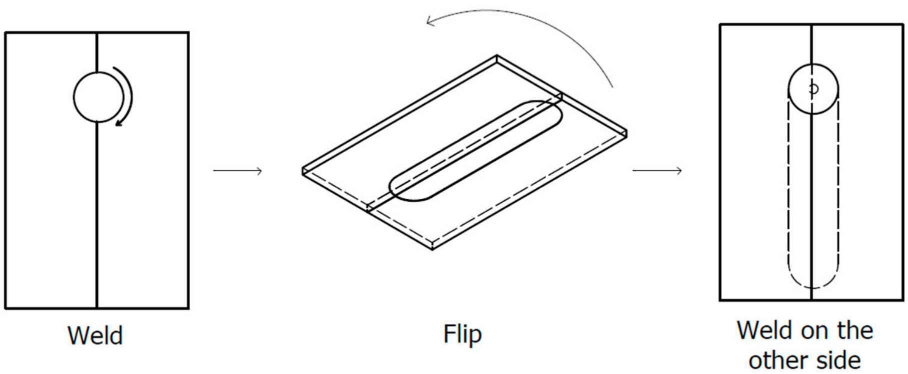

Figure 2. A simple schematic of weld–flip–weld configuration.

2.2. Selection of Parameters

Table 3 includes a comprehensive review of the key parameters employed by various authors in dissimilar FSW joints. It highlights details such as rotational speed, traverse speed, offset, and joint efficiency, which is defined as the strength of a welded joint compared with the minimum tensile strength of the base material [22], providing a comprehensive overview of the diverse approaches adopted in the research literature to achieve a high-quality weld.

Table 3. Parameters used in dissimilar FSW. Adapted from Refs. [12,13,15,16,23–48].

Aluminum Alloy	Copper	Thickness (mm)	Rotational Speed (RPM)	Traverse Speed (mm/min)	Offset (mm)	Joint Efficiency (%)	Reference
AA6061	DHP	3	1118	60	2	54.84%	[13]
AA6063	C26000	5	600	15	-	70.3%	[15]
AA5083	Pure	3	1400	120	0	96.4%	[16]
AA5083-H111	DHP R204	1	750	160	-	-	[48]
AA6082-T6	Pure	3	1000	200	1.9	-	[23]
AA6061	Pure	3	710	355	-	-	[12]
AA6063-T651	ETP	6.3	1500	50	2	40.5%	[24]
AA6061-T6	Pure	3	1300	70	-	-	[25]
AA6061-T6	Pure	2.8	900	63	0.5	-	[26]
AA6061-T6	C11000	3.1	1300	20	2	-	[27]
AA5754	C11000	3.175	950	50	0	78%	[28]
AA1060	Pure	5	600	100	2	44%	[29]
AA1060	Pure	3	1050	30	1	58%	[6]
AA6061-T651	Pure	6.3	1500	40	2	58%	[30]
AA1050-H14	Pure	6	800	125	1.4	85%	[31]
AA2024	Pure	2	948	85		70.2%	[32]
AA5083	Pure	5	800	40	1	69.4%	[33]
AA6061	Pure	6.3	1300	40	2	-	[34]
AA6061	C11000	3.2	1000	40	-	-	[35]
AA5083	Pure	3	825	32	-	-	[36]
AA5754	C11000	3.1	950	50	-	86%	[28]
AA6063	Pure	6	1800	20	-	-	[37]
AA6063	Pure	6	900	25	0	-	[38]
AA6063	HCP	3	800	20	0	-	[39]
AA6063	ETP	3	1200	15	0	-	[40]
AA5086	Pure	6.3	710	69	-	-	[41]
AA1350	Pure	3	1000	80	2	50%	[42]
AA5083	Pure	5	1200	30	-	58%	[43]
AA6061	B370	6	1100	120	-	-	[44]
AA5083	Pure	5	600	40	-	96%	[45]
AA1050-H14	Pure	2	1400	20	2	88%	[46]
AA1050-H14	Pure	2	1200	20	2	96%	[46]
AA5082	B36	2	1300	35	-	82%	[47]

Based on the conducted review, Figure 3 categorizes rotational and traverse speeds into two distinct groups: those falling below an efficiency of 70%, and those surpassing it. The selection of thicknesses ranging between 2 and 3 mm was driven by the requirements of the conducted trials and the CNC machine limitations. Figure 3 includes a summary of the reviewed parameter combinations and joint efficiency. The red triangles represent efficiencies below 70%, while the green circles indicate efficiencies above 70%, showing that most traverse speeds are between 20 mm/min and 85 mm/min and the range for rotational speed is 950 to 1400 RPM. It should be noted that higher rotational speeds tend to lead to higher efficiencies. Table 4 shows the parameters selected for the trials; the selection was initially based on the biographical review that is summarized in Table 3. Once the ranges of interest were identified, an experimental plan was proposed that used visual inspection of the joints as the first quality assessment. In the specific case of the feed rate in this experimental exercise, it was limited to a value that would be safe for the machine, similar to the use of flip welding to maintain the integrity of the equipment used.

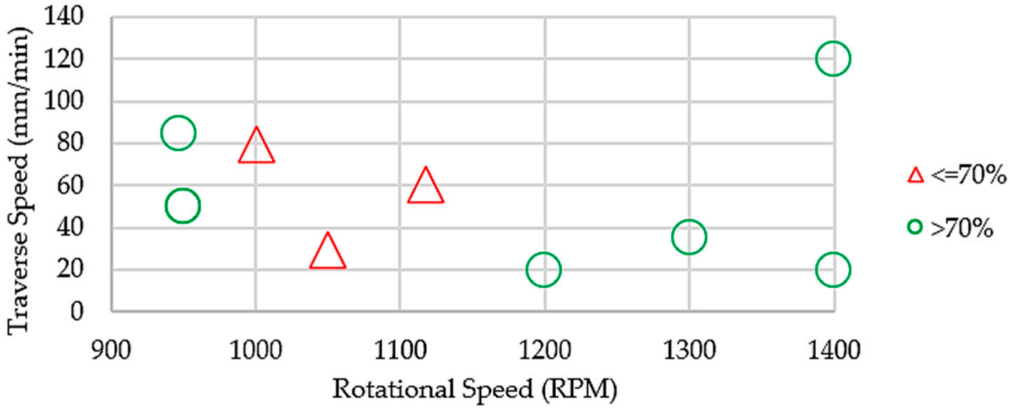

Figure 3. Summary of the reviewed parameter combinations and joint efficiency.

Offset is a parameter that is commonly used in dissimilar joints to account for differences in the properties of materials. Figure 4 includes a schematic of the offset selected for the trials. This tool movement compensates for variations in mechanical and thermal properties between workpieces, thereby controlling the distribution of heat in the joint [49]. In this case, and as some authors have suggested, the tool was moved towards the aluminum [42,50].

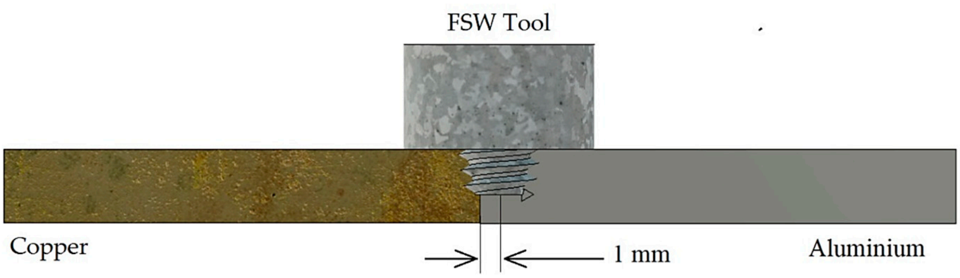

Figure 4. Schematic of the selected offset of 1mm towards the aluminum.

2.3. Non-Destructive Analysis

Within the context of FSW, there are standards and related information regarding non-destructive testing methods for joints welded with homogeneous materials. However, there is a noticeable disparity in the variety and accessibility of information regarding dissimilar joints [51]. This discrepancy underscores the need for further research and development in this area, particularly given the increasing prevalence of dissimilar material welding in various industrial applications. Given the materials employed in this scenario (copper and aluminum alloys), PAU testing emerged as a viable non-destructive technique. Its advantage over traditional ultrasonic inspections lies in its use of multiple wave-generating elements and its ability to concentrate and manipulate the ultrasonic beam without necessitating probe movement. This method facilitates image formation through the electronic manipulation of multiple ultrasonic elements to steer and focus the sound beam [52].

Table 4. Process parameters combinations selected per weld number.

Weld Number	Rotational Speed (RPM)	Traverse Speed (mm/min)	Offset (mm)
1	1000	40	1
2	1200	40	0
3	1000	40	0
4	1400	40	1
5	1200	40	1
6	1400	40	0
7	1400	40	1
8	1400	40	0

2.4. Tensile Testing

Tensile test specimens were prepared according to the ASTM E8 standard [53], as shown in the sketch in Figure 5a. It should be noted that the units are in mm. For each welding, three specimens were prepared, as shown in Figure 5b. To ensure the accuracy of the tests, each specimen underwent a surface polishing process to achieve a smooth and continuous surface. The polishing process was necessary to ensure a constant cross-sectional area in the gauge section.

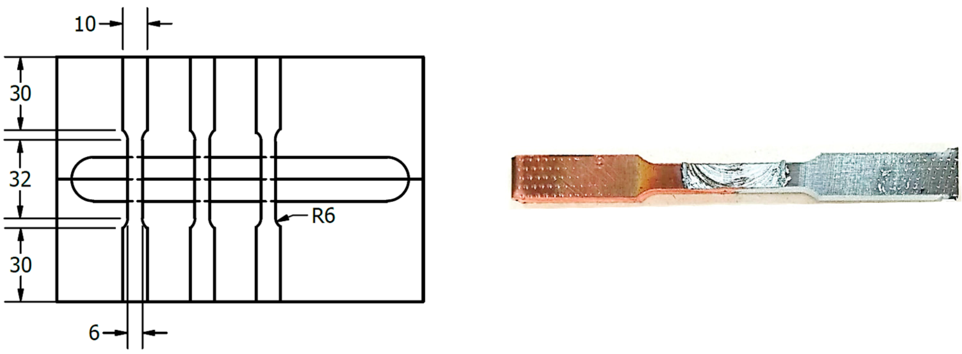

(**a**) (**b**)

Figure 5. (**a**) Tensile test specimens' location sketch in mm. (**b**) Aluminum–copper tensile test specimen.

To calculate the sample size, Montgomery's guidance was used, employing Equation (1) [54], where $Z_{\alpha/2}$ and Z_β are the z-scores according to the confidence level and the statistical power, respectively; σ is the standard deviation; and δ is the difference quantifying the magnitude of the effect that the study is designed to detect.

$$N = \frac{\left(Z_{\alpha/2}^2 + Z_\beta^2\right)\sigma^2}{\delta^2} \quad (1)$$

The expected sample size was calculated considering a confidence level of 95% and a statistical power of 80%. A preliminary test yielded a standard deviation of efficiency at 0.16, based on previous initial experimental results. Assuming a significant detectable difference (δ) in welding efficiency of 0.20, the calculated sample size necessary for each group of welds was approximately 3. It is noteworthy that a larger sample size would have been preferable; however, due to significant limitations, it was not feasible.

2.5. Electrical Conductivity Analysis

Due to the extensive use of dissimilar joints in the electrical industry, electrical conductivity testing was considered a key factor to be included in the analysis. The analysis was conducted using a specialized conductivity meter. This device directly measured the electrical conductivity of the material at various points along the weld line.

The assessment was performed at three different locations along the weld: when the FSW tool entered the workpiece (axis 1), when it advanced through the joint (axis 2), and when the FSW tool was extracted (axis 3), as shown in Figure 6.

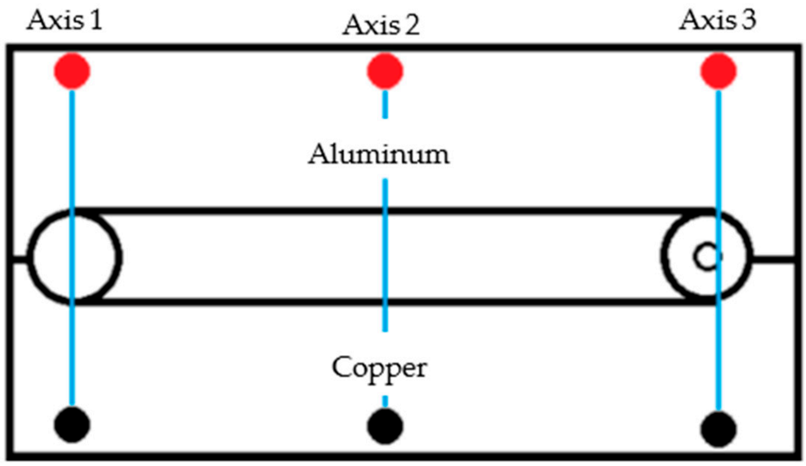

Figure 6. Locations for electrical conductivity measurements.

3. Results and Discussion

This section presents the outcomes of the NDT, tensile testing, electrical conductivity analysis, and other evaluations.

3.1. Phased-Array Ultrasound (PAU)

A phased-array ultrasound was conducted on eight plates corresponding to the welding executed. Non-destructive testing was conducted using the Phased Array General Electric equipment (Mentor UT model) equipped with a 32-crystal transducer (serial number 17I00CJH). The GE 20D00T4A transducer and software designed for measurements with a 32° crystal beam were utilized. Adjustment was performed using the calibration ladder with the serial number GE V39377. The PAU results can be seen in Figure 7.

Based on the measurements, it is noticeable that there are differences in densities between aluminum and copper. The aluminum side appears in darker green (Figure 7). After conducting non-destructive testing, it was observed that welds 1, 2, 3, 5, 7, and 8 had significant defects in the weld zone, ranging from 53 mm to 90 mm in length, where areas marked in red indicated lower density. Moreover, welds 1, 3, and 5 presented a continuous tunnel of approximately 90 mm in length, showing a lack of material along the joint. Welds 4 and 6 showed smaller indications of approximately 2 mm to 5 mm in length. It should be noted that these welds used a higher rotational speed (1400 RPM). The speed and offset were the same for welds 4 and 7 and welds 6 and 8, although it is worth mentioning some aspects that possibly contributed to this variability, such as tool temperature. It is important to mention that the objective of this non-destructive testing was to assess the integrity of the weld and understand the influence of the process parameters. Furthermore, it served as a means to identify defect-free sections suitable for tensile testing. In each instance, a minimum of one sample, and ideally three specimens per weld, were examined.

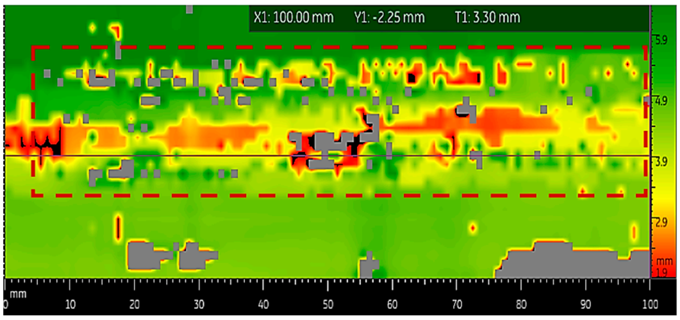

(**a**) Weld 1.

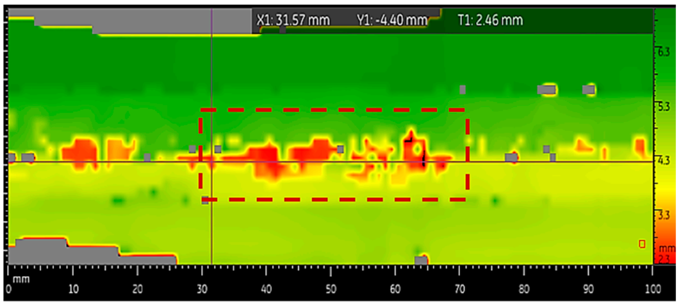

(**b**) Weld 2.

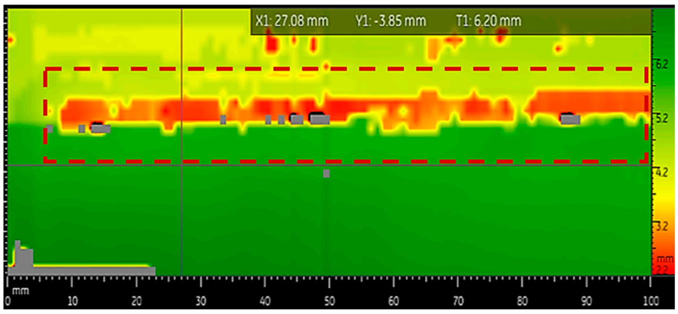

(**c**) Weld 3.

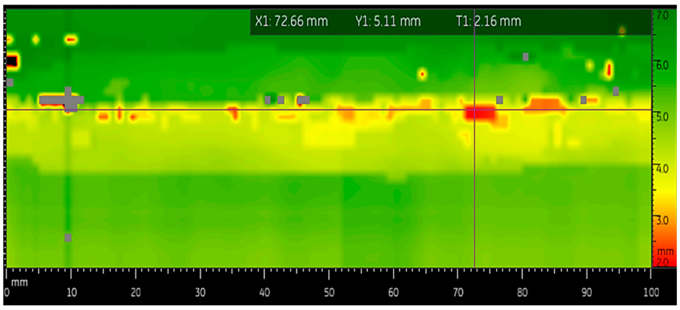

(**d**) Weld 4.

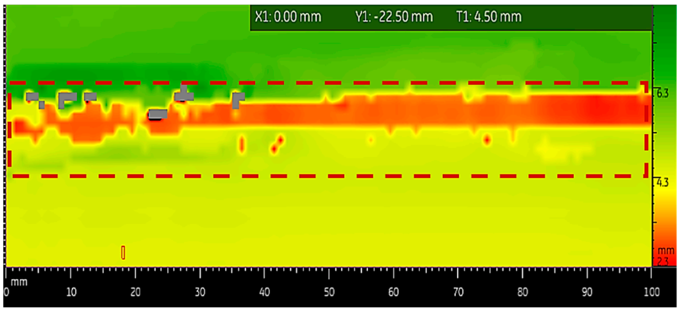

(**e**) Weld 5.

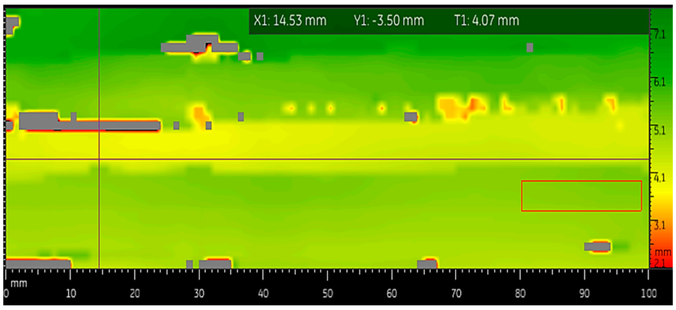

(**f**) Weld 6.

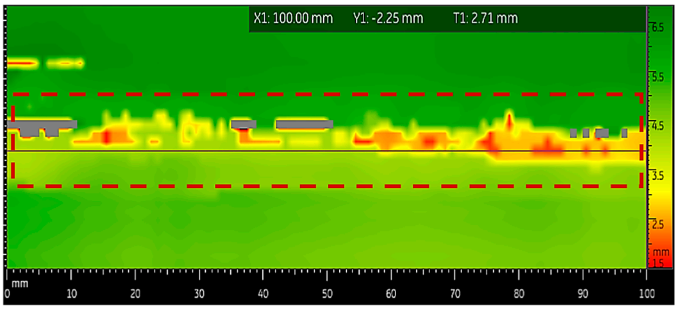

(**g**) Weld 7.

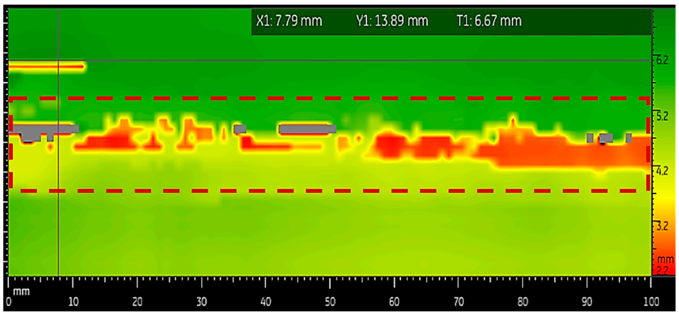

(**h**) Weld 8.

Figure 7. PAU results for welds (**a**) 1, (**b**) 2, (**c**) 3, (**d**) 4, (**e**) 5, (**f**) 6, (**g**) 7, and (**h**) 8.

3.2. Electrical Properties

Table 5 shows the electrical properties results, including the welds' resistance, resistivity, electrical conductivity, and % IACS.

As shown in Table 5, all the welds except weld 5 had an average % IACS higher than that of aluminum (39%), but in all cases, it was lower than that of copper. The best results were seen in weld 4, with 66.3%, which is also the soundest joint based on the PAU images. Weld 6 presented a higher uniformity across the three axes, with values of approximately 56.3% and a standard deviation of 4.4%.

Table 5. Electrical properties results.

Weld Number	Axes	Resistance (Ohm)	Resistivity (Ω.m)	Electrical Conductivity (S/m)	% IACS	Average
1	1	6.60×10^{-5}	3.37×10^{-8}	2.97×10^{7}	51.2%	58.2%
	2	6.20×10^{-5}	3.16×10^{-8}	3.16×10^{7}	54.5%	
	3	4.90×10^{-5}	2.50×10^{-8}	4.00×10^{7}	69.0%	
2	1	6.70×10^{-5}	3.42×10^{-8}	2.93×10^{7}	50.4%	39.5%
	2	1.07×10^{-4}	5.46×10^{-8}	1.83×10^{7}	31.6%	
	3	9.30×10^{-5}	4.74×10^{-8}	2.11×10^{7}	36.3%	
3	1	6.90×10^{-5}	3.52×10^{-8}	2.84×10^{7}	49.0%	49.8%
	2	5.70×10^{-5}	2.91×10^{-8}	3.44×10^{7}	59.3%	
	3	8.20×10^{-5}	4.18×10^{-8}	2.39×10^{7}	41.2%	
4	1	5.30×10^{-5}	2.70×10^{-8}	3.70×10^{7}	63.8%	66.3%
	2	4.10×10^{-5}	2.09×10^{-8}	4.78×10^{7}	82.4%	
	3	6.40×10^{-5}	3.27×10^{-8}	3.06×10^{7}	52.8%	
5	1	9.60×10^{-5}	4.90×10^{-8}	2.04×10^{7}	35.2%	35.8%
	2	9.40×10^{-5}	4.80×10^{-8}	2.09×10^{7}	36.0%	
	3	9.30×10^{-5}	4.74×10^{-8}	2.11×10^{7}	36.3%	
6	1	6.60×10^{-5}	3.37×10^{-8}	2.97×10^{7}	51.2%	56.3%
	2	5.70×10^{-5}	2.91×10^{-8}	3.44×10^{7}	59.3%	
	3	5.80×10^{-5}	2.96×10^{-8}	3.38×10^{7}	58.3%	
7	1	9.60×10^{-5}	4.90×10^{-8}	2.04×10^{7}	35.2%	49.3%
	2	5.30×10^{-5}	2.70×10^{-8}	3.70×10^{7}	63.8%	
	3	6.90×10^{-5}	3.52×10^{-8}	2.84×10^{7}	49.0%	
8	1	8.20×10^{-5}	4.18×10^{-8}	2.39×10^{7}	41.2%	55.5%
	2	5.60×10^{-5}	2.86×10^{-8}	3.50×10^{7}	60.3%	
	3	5.20×10^{-5}	2.65×10^{-8}	3.77×10^{7}	65.0%	

3.3. Tensile Testing

The SHIMADZU AGX-50kNvd machine was used for tensile testing, and the results are shown in Table 6. The mechanical efficiency of the welds was determined by comparing their mechanical properties to those of the base materials. The softer base material—in this case, AA 6061—served as the baseline for the calculation, with a tensile strength of 224 MPa. Although three samples per weld were planned initially, some of the specimens proved unsuitable for mechanical testing. Consequently, sound tensile specimens could not be obtained from welds 5, 7, and 8. The highest result was achieved for weld 4, with 75.1%.

Table 6. Tensile testing results obtained from SHIMADZU AGX-50kNvd machine.

Weld Number	Specimen	UTS (MPa)	Efficiency (%)
1	p1	125	55.8
2	p2	72.4	32.3
	p3	100.5	44.9
3	p1	57.7	25.8
4	p1	136.7	61.0
	p2	168.3	75.1
	p3	131.6	58.8
6	p1	65	29.0
	p2	96.7	43.2
	p3	110.3	49.2

Figure 8 includes a comparison of the process parameters (offset and rotational speed) with the resulting joint efficiency. The transverse speed was kept constant at 40 mm/min during the welding process.

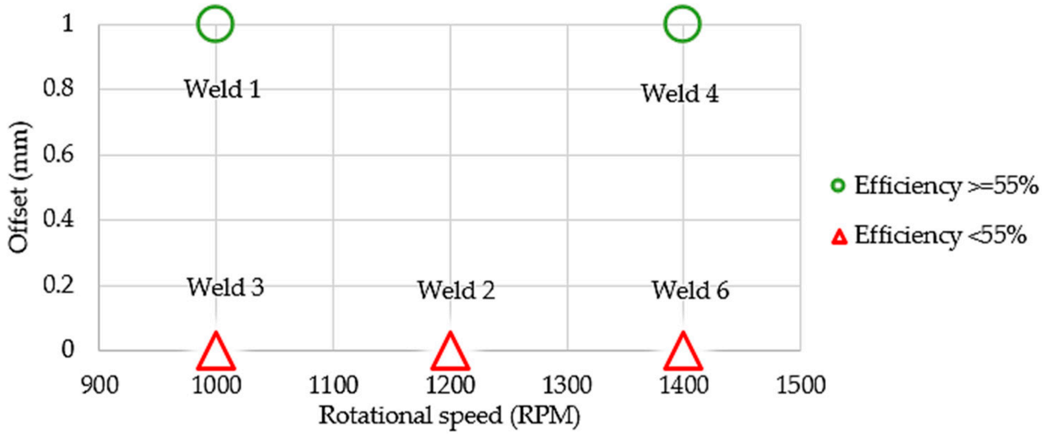

Figure 8. Comparison of process parameters and efficiency at 40 mm/min travel speed.

The data from Figure 8 suggests that the highest efficiencies were attained with a 1 mm offset. Conversely, joints with no offset, equivalent to 0 mm, yielded efficiencies below 55% and as low as 25.8%.

Statistical Analysis

A statistical analysis was conducted to evaluate the obtained results, which included both ANOVA and T-Student. It focused on welding groups 2, 4, and 6, as these were the only groups with more than one viable produced sample.

- Student's *t*-test

A T-Student test was conducted due to the study comprising fewer than 30 samples per group, which facilitated the computation of 95% confidence intervals for the sample efficiencies. As detailed in Table 7, the maximum standard deviation observed was 0.0847, which was deemed acceptable. The analysis revealed significant variance among the groups, with group 4 exhibiting both a higher mean and a wider confidence interval, indicating greater efficacy but also increased variability.

Table 7. The 95% confidence interval for weld groups 2, 4, and 6.

Weld Number	Quantity	Degrees of Freedom	Standard Deviation	Alpha Value	Width of Confidence Interval
2	3	2	0.0627	0.05	0.1558
4	3	2	0.0725	0.05	0.1801
6	3	2	0.0847	0.05	0.2104

- ANOVA

Table 8 displays the Analysis of Variance (ANOVA) results for welding groups 2, 4, and 6. The obtained F-value of 65.535 significantly surpassed the critical F-value of 5.1433, indicating a statistically significant difference in the efficiencies. This result could be improved by including additional tests to ensure the robustness of the study.

Table 8. ANOVA for weld groups 2, 4, and 6.

Source of Variation	Sum of Squares	Degrees of Freedom	Mean Squares	F-Value	Probability	Critical F-Value
Between Groups	0.1106	2	0.0553	65,535	∞	5.1433
Within Groups	0	6	0			
Total	0.1106	8				

3.4. Joint Efficiency and Electrical Conductivity

The previously obtained results were compared, recognizing that mechanical and electrical properties serve distinct purposes and can be influenced by various factors during the welding process. Figure 9 illustrates the average joint efficiency and % IACS for five parameter combinations. A higher % IACS, indicating superior electrical conductivity, typically correlates with higher efficiency, consistent with a continuous material capable of conducting electricity and withstanding mechanical forces more effectively.

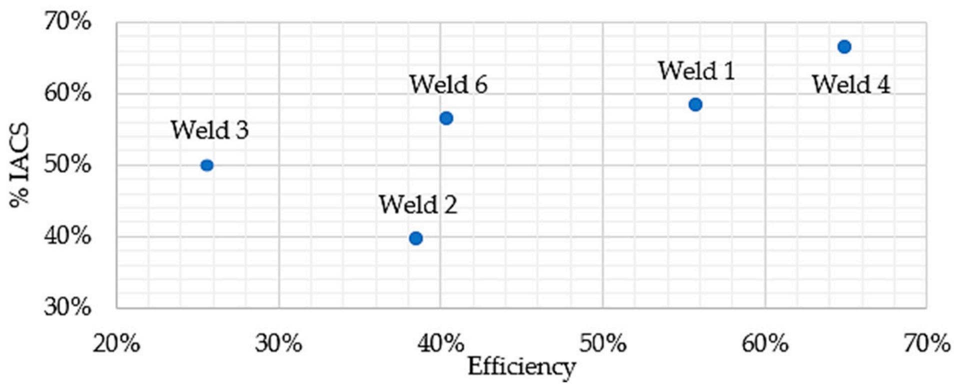

Figure 9. Efficiency compared with electrical properties.

3.5. Material Flow General Overview

Figure 10 includes a stereoscopic image from a weld executed at 1000 RPM and 40 mm/min (weld 1). In this figure, it is possible to observe a higher level of mixing with the use of offset, with an increase in material flow from the softest material—aluminum, in this case—to the most rigid. This observation is further confirmed in Figure 11 by the presence of lines indicating significant and heterogeneous plastic deformation on the aluminum side.

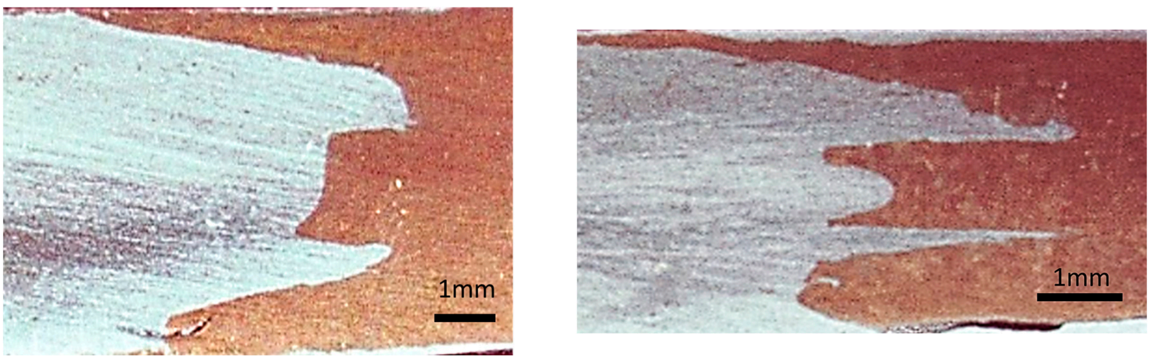

(a) **(b)**

Figure 10. Stereoscopic image of heterogeneous welds (a) without offset and (b) with offset.

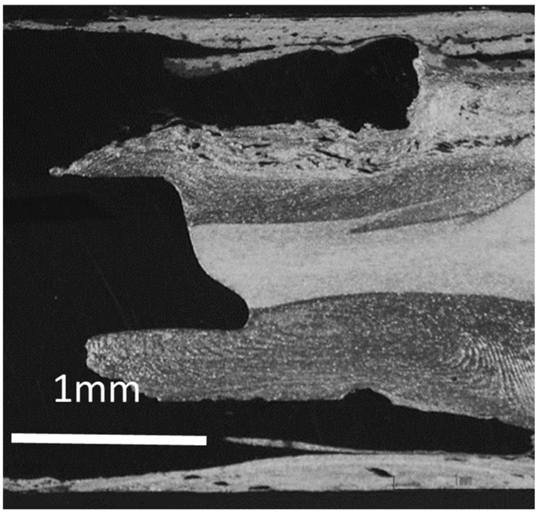

Figure 11. Heterogeneous weld microstructure; modified Keller etchant for the aluminum side.

4. Conclusions

The dissimilar joints executed with Friction Stir Welding (FSW) between aluminum AA6061-T6 and pure copper C11000 were investigated. Following a literature review focused on various techniques of aluminum–copper welding through FSW, a trend was observed: conditions leading to the highest efficiencies typically involve high rotation speeds and low traverse speeds. In order to select optimal parameters, experiments were conducted with rotation speeds ranging from 1000 RPM to 1400 RPM, and traverse speed of 40 mm/min. Additionally, the influence of offset was explored, varying between 0 mm and 1 mm towards the aluminum.

PAU inspection was utilized, enabling the detection of density variations in the welded regions, i.e., volumetric flaws. This information was used to accurately locate the specimens for tensile testing and compared them with electrical conductivity testing. The combined techniques provided an evaluation of joint soundness, facilitating a deeper understanding of welding parameter combinations and their effects on the mechanical and electrical properties of the weld. Considering the PAU inspection, welds 4 and 6 showed the best outcomes, including a lack of material areas of approximately 2 mm to 5 mm in length. In contrast, welds 3 and 5 show a continuous tunnel presented along the joint.

Analysis of the results from tensile tests revealed a trend towards higher mechanical strengths at higher rotation speeds, in line with the literature review findings. It was observed that combinations of 1400 RPM, 40 mm/min, and offset of 1 mm, achieved the highest joint efficiency, reaching approximately 75% (weld 4), underscoring the importance of the right parameter combinations in weld quality. Considering the evaluation of conductivity along the welds, the provided % IACS values aligned with the mechanical characterization findings. Notably, the best result (82.42%) was also obtained for weld 4. It should be noted that these results have coherence with the PAU testing result, in which weld 4 presented smaller indications compared with the other welds.

As a final conclusion, this article offers a literature review on dissimilar FSW of the selected pairs and the results of an experimental exercise that align closely with theoretical findings. It is worth highlighting the advantageous use of the weld–flip–weld technique for safeguarding the adapted welding equipment utilized in this project. However, it is crucial to acknowledge the notable variability observed in the results due to this technique and, as aforementioned, more data are necessary to support the observations which were not available in this study. It is also recommended to conduct a new series of tests employing full penetration welds from a single side. This approach will facilitate a focused analysis of this single variable and also validate the reported observations.

Author Contributions: Conceptualization, E.H. and M.C.S.; Methodology, E.H. and M.C.S.; Validation, E.H., M.C.S., Y.M. and J.H.C.; Formal analysis, E.H., M.C.S., Y.M. and J.H.C.; Investigation, E.H., M.C.S., Y.M. and J.H.C.; Resources, E.H. and M.C.S.; Data curation, E.H. and M.C.S.; Writing—original draft preparation, E.H. and M.C.S.; Writing—review and editing, E.H., M.C.S., Y.M. and J.H.C.; Supervision, E.H.; Project administration, E.H. All authors have read and agreed to the published version of the manuscript.

Funding: This research was funded by Universidad EIA in the project called "Development of solid-state heterogeneous seals of non-ferrous materials for the electrical and transport industries".

Data Availability Statement: The raw data supporting the conclusions of this article will be made available by the authors on request.

Conflicts of Interest: The authors declare no conflicts of interest.

References

1. Mishra, R.S.; Ma, Z.Y. Friction Stir Welding and Processing. *Mater. Sci. Eng. R Rep.* **2005**, *50*, 1–78. [CrossRef]
2. Rai, R.; De, A.; Bhadeshia, H.K.D.H.; DebRoy, T. Review: Friction Stir Welding Tools. *Sci. Technol. Weld. Join.* **2011**, *16*, 325–342. [CrossRef]
3. Mubiayi, M.P.; Titilayo, E.; Mamookho, M. *Current Trends in Friction Stir Welding (FSW) and Friction Stir Spot Welding (FSSW)*; Springer: Cham, Switzerland, 2019.
4. Mendes, N.; Neto, P.; Loureiro, A.; Moreira, A.P. Machines and Control Systems for Friction Stir Welding: A Review. *Mater. Des.* **2016**, *90*, 256–265. [CrossRef]
5. Busu, A.; Shamil Jaffarullah, M.; Yee Low, C.; Saiful Bahari Shaari, M.; Jaffar, A. A Review of Force Control Techniques in Friction Stir Process. *Procedia Comput. Sci.* **2015**, *76*, 528–533. [CrossRef]
6. Zhang, Q.Z.; Gong, W.B.; Liu, W. Microstructure and Mechanical Properties of Dissimilar Al–Cu Joints by Friction Stir Welding. *Trans. Nonferrous Met. Soc. China* **2015**, *25*, 1779–1786. [CrossRef]
7. Nandan, R.; DebRoy, T.; Bhadeshia, H.K.D.H. Recent Advances in Friction-Stir Welding-Process, Weldment Structure and Properties. *Prog. Mater. Sci.* **2008**, *53*, 980–1023. [CrossRef]
8. Taheri, H.; Kilpatrick, M.; Norvalls, M.; Harper, W.J.; Koester, L.W.; Bigelow, T.; Bond, L.J. Investigation of Nondestructive Testing Methods for Friction Stir Welding. *Metals* **2019**, *9*, 624. [CrossRef]
9. Mehta, K.P. A Review on Friction-Based Joining of Dissimilar Aluminum-Steel Joints. *J. Mater. Res.* **2018**, *3*, 78–96. [CrossRef]
10. Sathishkumar, G.B.; Sethuraman, P.; Chanakyan, C.; Sundaraselvan, S.; Arockiam, A.J.; Alagarsamy, S.V.; Elmariung, A.; Meignanamoorthy, M.; Ravichandran, M.; Jayasathyakawin, S. Friction Welding of Similar and Dissimilar Materials: A Review. *Sel. Peer-Rev. Under Responsib. Sci. Comm. Int. Virtual Conf. Sustain. Mater. (IVCSM-2k20)* **2021**, *81*, 208–211. [CrossRef]
11. Agapiou, J.S.; Carlson, B.E. Friction Stir Welding for Assembly of Copper Squirrel Cage Rotors for Electric Motors. *Procedia Manuf.* **2020**, *48*, 1143–1154. [CrossRef]
12. Mehta, K.P.; Badheka, V.J. A Review on Dissimilar Friction Stir Welding of Copper to Aluminum: Process, Properties, and Variants. *Mater. Manuf. Process.* **2016**, *31*, 233–254. [CrossRef]
13. Al-Jarrah, J.A.; Ibrahim, M.; Swalha, S.; Gharaibeh, N.S.; Al-Rashdan, M.; Al-Qahsi, D.A. Surface Morphology and Mechanical Properties of Aluminum-Copper Joints Welded by Friction Stir Welding. *Contemp. Eng. Sci.* **2014**, *7*, 219–230. [CrossRef]
14. Ahmadi, M.; Pahlavani, M.; Rahmatabadi, D.; Marzbanrad, J.; Hashemi, R.; Afkar, A. An Exhaustive Evaluation of Fracture Toughness, Microstructure, and Mechanical Characteristics of Friction Stir Welded Al6061 Alloy and Parameter Model Fitting Using Response Surface Methodology. *J. Mater. Eng. Perform.* **2022**, *31*, 3418–3436. [CrossRef]
15. Chowdhury, I.; Sengupta, K.; Maji, K.K.; Roy, S.; Ghosal, S. Investigation of Mechanical Properties of Dissimilar Joint of Al6063 Aluminium Alloy and C26000 Copper Alloy by Ultrasonic Assisted Friction Stir Welding. *Mater. Today Proc.* **2022**, *50*, 1527–1534. [CrossRef]
16. Karrar, G.; Galloway, A.; Toumpis, A.; Li, H.; Al-Badour, F. Microstructural Characterisation and Mechanical Properties of Dissimilar AA5083-Copper Joints Produced by Friction Stir Welding. *J. Mater. Res. Technol.* **2020**, *9*, 11968–11979. [CrossRef]
17. Gruber, S.; Stepien, L.; López, E.; Brueckner, F.; Leyens, C. Physical and Geometrical Properties of Additively Manufactured Pure Copper Samples Using a Green Laser Source. *Materials* **2021**, *14*, 3642. [CrossRef]
18. Eslami, N.; Harms, A.; Deringer, J.; Fricke, A.; Böhm, S. Dissimilar Friction Stir Butt Welding of Aluminum and Copper with Cross-Section Adjustment for Current-Carrying Components. *Metals* **2018**, *8*, 661. [CrossRef]
19. Yusof, F.; Firdaus, A.; Fadzil, M.; Hamdi, M. Ultra-Thin Friction Stir Welding (FSW) between Aluminum Alloy and Copper. In Proceedings of the 1st International Joint Symposium on Joining and Welding, Osaka, Japan, 6–8 November 2013; Elsevier: Amsterdam, The Netherlands, 2013; pp. 219–224.
20. Bakhtiari Argesi, F.; Shamsipur, A.; Mirsalehi, S.E. Dissimilar Joining of Pure Copper to Aluminum Alloy via Friction Stir Welding. *Acta Metall. Sin. (Engl. Lett.)* **2018**, *31*, 1183–1196. [CrossRef]
21. MatWeb Online Materials Information Resource. Available online: https://www.matweb.com/ (accessed on 21 December 2023).

22. *ISO 25239-4:2011*; Friction Stir Welding—Aluminium 4: Specification and Qualification of Welding Procedures. ISO: Geneva, Switzerland, 2011.
23. Galvão, I.; Loureiro, A.; Verdera, D.; Gesto, D.; Rodrigues, D.M. Influence of Tool Offsetting on the Structure and Morphology of Dissimilar Aluminum to Copper Friction-Stir Welds. *Metall. Mater. Trans. A Phys. Metall. Mater. Sci.* **2012**, *43*, 5096–5105. [CrossRef]
24. Mehta, K.P.; Badheka, V.J. Influence of Tool Pin Design on Properties of Dissimilar Copper to Aluminum Friction Stir Welding. *Trans. Nonferrous Met. Soc. China (Engl. Ed.)* **2017**, *27*, 36–54. [CrossRef]
25. Prabhu, L.; Satish Kumar, S. Tribological Characteristics of FSW Tool Subjected to Joining of Dissimilar AA6061-T6 and Cu Alloys. *Mater. Today Proc.* **2020**, *33*, 741–745. [CrossRef]
26. Sharma, N.; Khan, Z.A.; Siddiquee, A.N.; Shihab, S.K.; Wahid Atif, M. Effect of Process Parameters on Microstructure and Electrical Conductivity during FSW of Al-6101 and Pure Copper. *Certain. Distance Degree Based Topol. Indices Zeolite LTA Framew.* **2018**, *5*, 11–14. [CrossRef]
27. García-Navarro, D.; Ortiz-Cuellar, J.C.; Galindo-Valdés, J.S.; Gómez-Casas, J.; Muñiz-Valdez, C.R.; Rodríguez-Rosales, N.A. Effects of the FSW Parameters on Microstructure and Electrical Properties in Al 6061-T6- Cu C11000 Plate Joints. *Crystals* **2021**, *11*, 21. [CrossRef]
28. Akinlabi, E.T. Effect of Shoulder Size on Weld Properties of Dissimilar Metal Friction Stir Welds. *J. Mater. Eng. Perform.* **2012**, *21*, 1514–1519. [CrossRef]
29. Xue, P.; Ni, D.R.; Wang, D.; Xiao, B.L.; Ma, Z.Y. Effect of Friction Stir Welding Parameters on the Microstructure and Mechanical Properties of the Dissimilar Al-Cu Joints. *Mater. Sci. Eng. A* **2011**, *528*, 4683–4689. [CrossRef]
30. Emamian, S.; Awang, M.; Hussai, P.; Meyghani, B.; Zafar, A. Influences of Tool Pin Profile on the Friction Stir Welding of AA6061. *ARPN J. Eng. Appl. Sci.* **2016**, *11*, 12258–12261.
31. Ólafsson, D.; Vilaça, P.; Vesanko, J. Multiphysical Characterization of FSW of Aluminum Electrical Busbars with Copper Ends. *Weld. World* **2020**, *64*, 59–71. [CrossRef]
32. Khajeh, R.; Jafarian, H.R.; Seyedein, S.H.; Jabraeili, R.; Eivani, A.R.; Park, N.; Kim, Y.; Heidarzadeh, A. Microstructure, Mechanical and Electrical Properties of Dissimilar Friction Stir Welded 2024 Aluminum Alloy and Copper Joints. *J. Mater. Res. Technol.* **2021**, *14*, 1945–1957. [CrossRef]
33. Rasaee, S.; Mirzaei, A.H.; Almasi, D.; Hayati, S. A Comprehensive Study of Parameters Effect on Mechanical Properties of Butt Friction Stir Welding in Aluminium 5083 and Copper. *Trans. Indian Inst. Met.* **2018**, *71*, 1553–1561. [CrossRef]
34. Mehta, K.P.; Badheka, V.J. Effects of Tilt Angle on the Properties of Dissimilar Friction Stir Welding Copper to Aluminum. *Mater. Manuf. Process.* **2016**, *31*, 255–263. [CrossRef]
35. Bisadi, H.; Tavakoli, A.; Tour Sangsaraki, M.; Tour Sangsaraki, K. The Influences of Rotational and Welding Speeds on Microstructures and Mechanical Properties of Friction Stir Welded Al5083 and Commercially Pure Copper Sheets Lap Joints. *Mater. Des.* **2013**, *43*, 80–88. [CrossRef]
36. Montes-González, F.A.; Rodríguez-Rosales, N.A.; Ortiz-Cuellar, J.C.; Muñiz-Valdez, C.R.; Gómez-Casas, J.; Galindo-Valdés, J.S.; Gómez-Casas, O. Experimental Analysis and Mathematical Model of Fsw Parameter Effects on the Corrosion Rate of Al 6061-T6-Cu C11000 Joints. *Crystals* **2021**, *11*, 294. [CrossRef]
37. View of Feasibility Study of Friction Stir Welding of Dissimilar Metals between 6063 Aluminium Alloy and Pure Copper. Available online: https://ph01.tci-thaijo.org/index.php/nuej/article/view/70365/72339 (accessed on 15 May 2022).
38. Christon, L.; Samuel, K. Balachandar Experimental Investigation on Friction Stir Welded Aluminium Alloy (6063-O)–Pure Copper Joint-Document-Gale Academic OneFile. Available online: https://go.gale.com/ps/i.do?id=GALE%7CA466052674&sid=googleScholar&v=2.1&it=r&linkaccess=abs&issn=19950772&p=AONE&sw=w&userGroupName=anon~5b1f7ab6 (accessed on 15 May 2022).
39. Bhattacharya, T.K.; Das, H.; Pal, T.K. Influence of Welding Parameters on Material Flow, Mechanical Property and Intermetallic Characterization of Friction Stir Welded AA6063 to HCP Copper Dissimilar Butt Joint without Offset. *Trans. Nonferrous Met. Soc. China (Engl. Ed.)* **2015**, *25*, 2833–2846. [CrossRef]
40. Panaskar, N.; Terkar, R. Effect of Process Parameters on Defect Features and Mechanical Performance of Friction Stir Lap Welded AA6063 and ETP Copper Joints. *Int. J. Recent Technol. Eng.* **2019**, *8*, 879–883. [CrossRef]
41. Al-Roubaiy, A.O.; Nabat, S.M.; Batako, A.D.L. Experimental and Theoretical Analysis of Friction Stir Welding of Al–Cu Joints. *Int. J. Adv. Manuf. Technol.* **2014**, *71*, 1631–1642. [CrossRef]
42. Li, X.W.; Zhang, D.T.; Qiu, C.; Zhang, W. Microstructure and Mechanical Properties of Dissimilar Pure Copper/1350 Aluminum Alloy Butt Joints by Friction Stir Welding. *Trans. Nonferrous Met. Soc. China* **2012**, *22*, 1298–1306. [CrossRef]
43. Ghangas, G.; Goyat, V.; Sirohi, S.; Sharma, S.K.; Dhull, S. Investigation for Mechanical Properties of Dissimilar Friction Stir Welded Joints of AA5083 and Pure Cu. *Mater. Today Proc.* **2022**, *56*, 77–81. [CrossRef]
44. Kadian, A.K.; Biswas, P. The Study of Material Flow Behaviour in Dissimilar Material FSW of AA6061 and Cu-B370 Alloys Plates. *J. Manuf. Process.* **2018**, *34*, 96–105. [CrossRef]
45. Fotoohi, Y.; Rasaee, S.; Bisadi, H.; Zahedi, M. Effect of Friction Stir Welding Parameters on the Mechanical Properties and Microstructure of the Dissimilar Al5083–Copper Butt Joint. *Proc. Inst. Mech. Eng. Part L J. Mater. Des. Appl.* **2014**, *228*, 334–340. [CrossRef]

46. Khodir, S.A.; Ahmed, M.M.Z.; Ahmed, E.; Mohamed, S.M.R.; Abdel-Aleem, H. Effect of Intermetallic Compound Phases on the Mechanical Properties of the Dissimilar Al/Cu Friction Stir Welded Joints. *J. Mater. Eng. Perform.* **2016**, *25*, 4637–4648. [CrossRef]
47. Afsari, A.; Heidari, S.; Jafari, J. Evaluation of Optimal Conditions, Microstructure, and Mechanical Properties of Aluminum to Copper Joints Welded by FSW. *J. Mod. Process. Manuf. Prod.* **2020**, *9*, 61–81.
48. Galvão, I.; Verdera, D.; Gesto, D.; Loureiro, A.; Rodrigues, D.M. Analysing the Challenge of Aluminum to Copper FSW. In Proceedings of the 9th International Symposium on Friction Stir Welding, Huntsville, AL, USA, 15–17 May 2012.
49. Ghiasvand, A.; Kazemi, M.; Mahdipour Jalilian, M.; Ahmadi Rashid, H. Effects of Tool Offset, Pin Offset, and Alloys Position on Maximum Temperature in Dissimilar FSW of AA6061 and AA5086. *Int. J. Mech. Mater. Eng.* **2020**, *15*, 1–14. [CrossRef]
50. Bakkiyaraj, M.; Bernard, S.S.; Saikrishnan, G.; Guruyogesh, S.; Guruprasanna, T.G.; Dineshkumar, K. Effect of Tool Offset Condition on Mechanical and Metallurgical Properties of FSW Dissimilar Al-Cu Joint. In Proceedings of the Materials Today: Proceedings; Elsevier Ltd.: Amsterdam, The Netherlands, 2020; Volume 43, pp. 824–827.
51. Akinlabi, E.T.; Levy, A.C.S.; Akinlabi, S.A. Non-Destructive Testing of Dissimilar Friction Stir Welds. In Proceedings of the World Congress on Engineering, London, UK, 4–6 July 2012.
52. Mandache, C.; Levesque, D.; Dubourg, L.; Gougeon, P. Non-Destructive Detection of Lack of Penetration Defects in Friction Stir Welds. *Sci. Technol. Weld. Join.* **2012**, *17*, 295–303. [CrossRef]
53. ASTM. E8 Standard Test Methods of Tension Testing of Metallic Materials. In *Annual Book or ASTM Standards*; American Society for Testing and Materials: Montgomery, PA, USA, 2024; Volume 3.01.
54. Montgomery, D.C. *Design and Analysis of Experiments*, 9th ed.; John Wiley & Sons: Hoboken, NJ, USA, 2022.